

See discussions, stats, and author profiles for this publication at: <https://www.researchgate.net/publication/317690774>

Ground level gamma-ray and electric field enhancements during disturbed weather: Combined signatures from convective clouds, lightning and rain

Article in *Atmospheric Research* · June 2017

DOI: 10.1016/j.atmosres.2017.06.012

CITATION

1

READS

178

4 authors, including:



Yuval Reuveni

Eastern R&D Center/Ariel University

24 PUBLICATIONS 56 CITATIONS

[SEE PROFILE](#)



Yoav Yair

Interdisciplinary Center Herzliya

189 PUBLICATIONS 1,999 CITATIONS

[SEE PROFILE](#)



Gideon Steinitz

Geological Survey of Israel

137 PUBLICATIONS 2,607 CITATIONS

[SEE PROFILE](#)

Some of the authors of this publication are also working on these related projects:



Diurnal E-field changes on mountains [View project](#)



A new approach for monitoring the 27-day solar rotation using VLF radio signals on the Earth's surface [View project](#)



Ground level gamma-ray and electric field enhancements during disturbed weather: Combined signatures from convective clouds, lightning and rain



Yuval Reuveni^{a,b,c,*}, Yoav Yair^c, Colin Price^d, Gideon Steinitz^e

^a Department of Mechanical Engineering & Mechatronics, Ariel University, Ariel, Israel

^b Eastern R & D Center, Ariel, Israel

^c School of Sustainability, Interdisciplinary Center (IDC) Herzliya, Herzliya, Israel

^d Department of Geosciences, Tel Aviv University, Ramat Aviv, Israel

^e Geological Survey of Israel, Jerusalem, Israel

ABSTRACT

We report coincidences of ground-level gamma-ray enhancements with precipitation events and strong electric fields typical of thunderstorms, measured at the Emilio Segre Cosmic Ray observatory located on the western slopes of Mt. Hermon in northern Israel. The observatory hosts $2 \times 2''$ NaI(Tl) gamma ray scintillation detectors alongside a vertical atmospheric electric field (E_z) mill and conduction current (J_z) plates. During several active thunderstorms that occurred near the Mt. Hermon station in October and November 2015, we recorded prolonged periods of gamma ray enhancements, which lasted tens of minutes and coincided with peaks both in precipitation and the vertical electric field. Two types of events were detected: slow increase (up to ~ 300 min) of atmospheric gamma ray radiation due to radon progeny washout (or rainout) along with minutes of E_z enhancement, which were not associated with the occurrences of nearby CG lightning discharges. The second type showed 30 min bursts of gamma rays, coinciding with minutes of E_z enhancement that closely matched the occurrences of nearby CG lightning discharges, and are superimposed on the radiation from radon daughters washed out to near surface levels by precipitation. We conclude that a superposition of accelerated high energy electrons by thunderstorm electric fields and radon progeny washout (or rainout) explains the relatively fast near surface gamma-ray increase, where the minutes-scale vertical electric field enhancement are presumably caused due to nearby convective clouds. Our results show that the mean exponential half-life depletion times of the residual nuclei produced during events without lightning occurrences were between ~ 25 – 65 min, compared to ~ 55 – 100 min when lightning was present, indicating that different types of nuclei were involved.

1. Introduction

The levels of atmospheric gamma-ray radiation near the ground are determined by the natural local concentrations of radioactive agents such as ^{222}Rn , which percolates from uranium bearing minerals in the crust. The flux of Radon atoms is related to content of U-bearing minerals, the emanation of radon and the porosity of the soil – all of which can vary significantly between locations (Mercier et al., 2009). The natural background levels at any given place are also a function of the meteorological conditions. These levels are monitored for public-health reasons, but also in order to give early-warning in case of nuclear accidents and intentional terror attacks. Deviations from the background pattern of gamma-ray levels are related to precipitation processes and have been used to evaluate rain age (Greenfield et al., 2008). The increase in near surface gamma-ray levels is mainly due to the activity of

radio nuclides such as ^{214}Pb and ^{214}Bi whose half-lives are 26.8 and 19.7 min, respectively, being scavenged by precipitation particles (rain drops or snow crystals), a well-known effect thoroughly discussed in the literature (Fujinami, 1996; Horng and Jiang, 2004; Livesay et al., 2014). The increase can be from a few to tens of percent compared to the background levels and depends on the rainfall rate (Takeyasu et al., 2006). For example, Burnett et al. (2010) reported gamma radiation levels exceeding by 125% compared with the mean background value in 9 distinct events of heavy precipitation near the Atomic Weapon Establishment site in Aldermaston, UK. They reported no correlation between the amount of rainfall and the dose rate increase, and the effect decreased back to normal values in 1–2 h. Recently, Hirouchi et al. (2014) reported a method for estimating the surface concentrations of the decay products in relation with gamma dose rate changes.

There are also seasonal patterns in the gamma-ray levels, related to

* Corresponding author at: Department of Mechanical Engineering & Mechatronics, Ariel University, Ariel, Israel.
E-mail address: yuvalr@ariel.ac.il (Y. Reuveni).

the geographical location and weather patterns (Inomata et al., 2007). Another source for observed increases in gamma-ray levels at the surface is attributed to thunderstorm and lightning activity (Greenfield et al., 2003; Ringuette et al., 2013). This mechanism involves the acceleration of protons by the strong electric fields within and below thunderstorms, which interact with the major components of air (nitrogen, oxygen, argon and carbon) and are decelerated to produce various types of radionuclides and brehmsstrahlung radiation (Greenfield et al., 2003). These are then transported downwards to the surface and deplete with exponential half-life depletion times of the order of ~ 55 min (see the Appendix in Greenfield et al., 2003 for details). Tsuchiya et al. (2011) also reported significant gamma-ray signals with minutes-scale duration and energy spectra extended to 10 MeV, and attributed these enhancements as products of relativistic electrons via brehmsstrahlung. An alternative explanation for short-lived (\sim few minutes) Thunderstorms Ground Enhancements (TGEs) of gamma-ray intensity observed at the surface was offered by Chilingarian and Mkrtchyan (2012) and Chilingarian (2014) who identified the Lower Positive Charge Center (LPCR) in thunderclouds as the acceleration agent. They attribute the rapid changes in the counts of gamma-rays at the surface to acceleration and multiplication of the stable background fluxes of secondary cosmic rays by the positive electric fields (i.e. E [kV m^{-1}] is directed away from the earth), specifically of downward moving electrons.

In this paper we present results from one year of measurements in northern Israel focused on two months of observations that include several precipitation and lightning events, when clear deviations from background values of the electric field and gamma-ray counts were observed. Section 2 presents the instruments and observation site, Section 3 describes the results where we distinguish between rain events with lightning and with rain only, and in Section 4 we conclude and discuss the coincidences, offering possible mechanisms.

2. Instruments

The Emilio Segre Cosmic-Ray observatory is located on Mount Hermon, near the triple border between Israel, Syria and Lebanon, ($33^{\circ}18'N$ $35^{\circ}47.2'E$) at an altitude ~ 2020 m MSL (Fig. 1). The mountain is steep and experiences strong winds and harsh weather conditions, especially in winter. The observatory is located on a small hill on the western flank of the mountain, and functions as part of the global neutron monitor network and records cosmic ray fluxes by using standard 6NM-64 detectors. It also measures basic meteorological parameters such as pressure, relative humidity, temperature and wind velocity. For monitoring the fair-weather electric field we used a CS110 electric field meter by Campbell Scientific Company, which measures the vertical component of the electric field (E_z) at a sampling frequency of 1 Hz. It is placed on top of a 2 m high mast that is attached to a 1-m high heavy tripod. For measuring the vertical conduction current density we used the Geometrical Displacement and Conduction Current Sensor (GDACCS), composed of two equal-area metal plates with a sampling frequency of 10 Hz (Bennett and Harrison, 2008; Elhalel et al., 2014). The meteorological parameters are obtained from an automatic weather station with 1 min resolution, but rain is collected at a separate station at a lower altitude (near the base-camp funicular station), a vertical separation of 500 m from the site. Rain gauge data are available at 30-min resolution, and although not measured at the Hermon site itself, the data represent the fact that it rained on the mountain (in reality, one can expect larger values of precipitation as we ascend higher up on the mountain). The detection of temporal variation of gamma radiation was achieved by using gamma detectors with $2 \times 2''$ NaI(Tl) scintillation detectors (PM-11; Rotem Industries Inc., Israel) tuned to the energy range of 50–3000 keV (Zafir et al., 2011), sampling at 15-min resolution. The PM-11 is placed vertically on the local ground and a Pb shield is located above it, within the local observatory facility. This configuration leads to preferred detection of gamma rays

from near surface air lateral to the detector.

Lightning data were obtained from the World Wide Lightning Location Network (WWLLN) and from the Israel Electrical Corporation (IEC), operating the Israel Lightning Detection Network (ILDN). The WWLLN determines the locations of lightning strokes based on the time of group arrival of at least 5 sensors, and normally only ~ 15 – 30% of strokes detected by one sensor are detected by 5 or more sensors. The strokes that are detected are usually the stronger ones, and recent studies indicate the WWLLN average global detection efficiency for strokes with peak currents > 30 kA is approximately 30% (Zheng et al., 2016). The ILDN system consists of 11 LPATS (based on time of arrival system) and IMPACT (based on both time of arrival along with magnetic direction and signal amplitude finding system) sensors (Cummins and Krider, 1998) distributed over the entire country from the Golan Heights to the Gulf of Eilat. Within the land area of Israel the stroke detection efficiency is $> 80\%$, and it decreases with distance from the network center (Tel-Aviv area). The system registers cloud-to-ground strokes with a time accuracy better than 1 ms, where flashes with a current between 0 and $+ 10$ kA are automatically filtered out, being treated as intra-cloud flashes (Shalev et al., 2011).

3. Observations

The data acquisition of the surface electric field (E_z) at Mt. Hermon site is maintained as long as weather condition allows, because from December through March the mountain is completely covered in snow (Fig. 1c), sometimes to a depth of several meters. After spring melt, measurements resume continuously from April through late November. The electric field (E_z) at any given place is affected by the local atmospheric conductivity, space charge density close to ground, global lightning activity and ionospheric conditions (Elhalel et al., 2014). Therefore, the diurnal variation curve of E_z has a predictable shape depending on the location of measurement. The average E_z value at Mt. Hermon is a downward-pointing negative field $\sim 290 \text{ Vm}^{-1}$ and fluctuates between 220 and 600 Vm^{-1} (Fig. 2a red rectangle close-up). It exhibits a seasonal dependence reflecting changes in the local sunrise hour, as well as differences in global lightning activity. The background diurnal variation of the fair weather electric field at Mt. Hermon was investigated by Yaniv et al. (2017). It exhibits the pattern of global thunderstorm activity of the Carnegie Curve (Harrison, 2013) with an additional early morning peak typical of mountainous regions, likely due to the anabatic (upslope) winds transporting aerosols that are reducing the conductivity (thus increasing the E_z) from lower areas in the Damascus plateau in the east and the Hula valley in the west. The gamma-ray background levels at Mt. Hermon also exhibit variations consisting of diurnal and multi-day signals, likely caused by changes in Radon (^{222}Rn) concentrations in the local lowermost atmosphere (Fig. 2b). The diurnal variations show a 24-h periodicity, with an average count rate of 220–230 counts/15 min (Fig. 2c).

We now focus our attention on a series of observations in October–November 2015, when several precipitation episodes occurred in succession over the station. We distinguish between those events that exhibited lightning activity and those that were not accompanied by electrical activity, in the manner reviewed by Bennett and Harrison (2007) that separated between shower and non-shower clouds. The fact that Mt. Hermon is located ~ 2200 m above sea level implies a small vertical separation between cloud-base and the instruments, and so the travel-time of raindrops is just a few minutes at most. Table 1 summarizes 13 distinct events that are analyzed in this study.

3.1. Events of rain with no lightning

On October 7–9th 2015 there were eight distinct rain episodes registered by the rain gauge at the lower funicular station, all of which were accompanied by disturbances in the electric field and deviations from the gamma-ray background values. Based on tephigrams from the

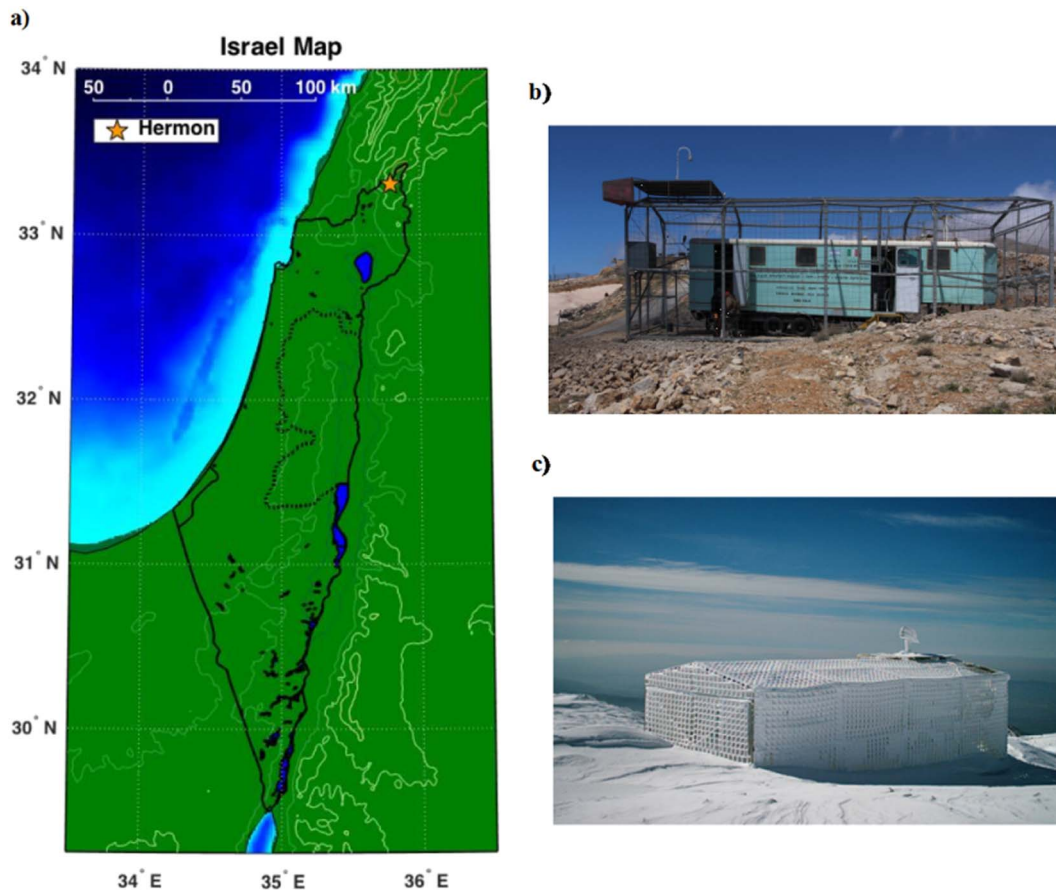


Fig. 1. a). Israel map showing the Mt. Hermon observation site location (orange star), where the Emilio Segre Observatory Israel (ESOI) is located. b). The observatory during a typical summer time. c). The observatory during winter time.

Bet-Dagan (Israeli Meteorological Service headquarters, 12 km east of Tel-Aviv) sounding we conclude that in all eight events the rain was from stratiform clouds. Fig. 3 shows the time series of the rainfall rate [mm/h], the vertical component of the electric field [V/m] and the gamma-ray counts [15 min^{-1}]. These episodes had weak rain-rates, of the order $< 5 \text{ mm/h}$, implying non-convective type of rain. The gamma-ray counts in all these events exhibit clear increase simultaneously or within a few minutes after rain was measured at the lower funicular gauge. The average time of gamma increase relative to background levels was $\sim 105 \text{ min}$. The extracted exponential half-life depletion time of the gamma-ray counts back to background levels was $\sim 49 \text{ min}$, suggesting that radon-daughter progenies were washed out by the rain from higher levels toward the surface (Burnett et al., 2010; Greenfield et al., 2008). The rather low rain-rate suggests that we see the gradual wash-out of radon daughters by the rain, because weaker rain-rates enable longer times for the scavenging of the radon decay products from the air as they travel toward the ground.

The electric field exhibited sharp polarity reversals and intensification, up to maximum values of 3.5 kV/m . Such strong fields are a result of the sharp reduction in the conductivity due to the presence of drops to which charged particles are attached (we compute σ from the vertical current density by applying Ohm's law, not shown). The polarity reversal is likely due to the fact that cloud-base above the sensor is charged negatively as is often found in electrical shower clouds. This effect was reported and modeled by Bennett and Harrison (2007). To exemplify the temporal evolution of this type of events we present an example from October 8–9, 2015 (Fig. 4). During these 24 h there were three distinct rain episodes, and in each one a clear departure from background values was observed in gamma-ray counts and measured E_z values (Fig. 5(a), (c) and (e)). The computed exponential half-life decay

times (Fig. 5(b), (d) and (f)) showing excellent fit ($R^2 > 0.96$) to radioactive depletion curves with exponential half-lives depletion of 64.8 (b), 24.8 (d) and 55.4 (f) minutes. Exponential half-lives depletion times represent the superposition of activity of radionuclides ^{214}Pb and ^{214}Bi being scavenged by the rain (Fujinami, 1996). The electric field increased up to 2000 V/m on a time scale of a few minutes and returned to fair weather values (of the order $\sim 300 \text{ V/m}$) within minutes after the rain ceased.

3.2. Events of rain with lightning

Between October 25th and November 17, 2005 there were five distinct gamma-ray burst episodes accompanied by minutes-scale E_z enhancement, which closely matched the occurrences of near-by CG lightning discharges, and were also superimposed with the radiation from radon daughters scavenging by precipitation. These episodes (Fig. 6) exhibited weak rain-rates, of the order $\sim 5 \text{ mm/h}$. The gamma-ray counts in all events show clear increases simultaneously with, or a few minutes after, rain was measured at the lower funicular gauge. The average time of gamma-ray increase relative to background levels was $\sim 30 \text{ min}$, and the extracted mean exponential half-lives depletion time of the gamma-ray counts to background levels was $\sim 79 \text{ min}$. The electric field exhibited sharp polarity reversals and increases, up to maximum values of 22.5 kV/m . Nearby (within an area of $60 \times 60 \text{ km}$ centered around Mt. Hermon) CG lightning discharges were detected by both the WWLNN and ILDN systems and were coincided with the minutes-scale E_z enhancements.

To exemplify the temporal evolution of such events we present an example from the convective event on October 25, 2015 (Fig. 7a) which started a day earlier as a trough extending from south along the Red-Sea

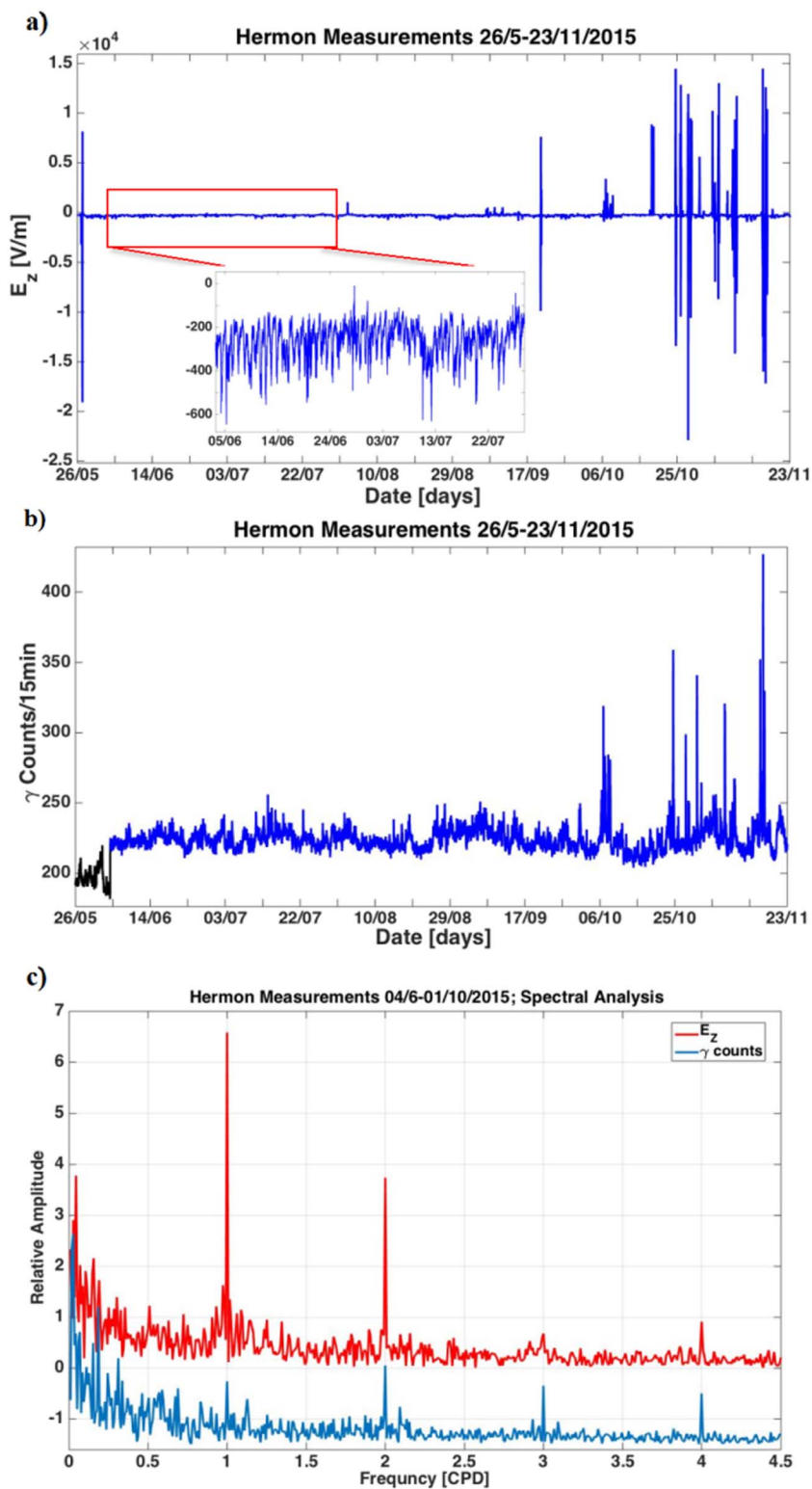


Fig. 2. Mount Hermon E_z and gamma-ray measurements between 26/5–23/11/2015. a). E_z time series data. Average E_z value is a downward-pointing negative field is 290 Vm^{-1} and fluctuating between 220 and 600 Vm^{-1} (red rectangle close-up) and it exhibits a seasonal dependence reflecting changes in the local sunrise hour, as well as differences in global lightning activity. b). Gama-ray time series data. Black line represents the period which a $20 \times 20 \times 5 \text{ cm}$ Pb plate shields it from direct gamma radiation from below along with the Pb shield located above, and the blue line represent the period without the Pb plates placed below the PM-11 detector. The gamma-ray background levels also exhibit variations consisting of diurnal and multi-day signals, likely caused by Radon (^{222}Rn) concentrations in the local lowermost atmosphere. c). E_z and gamma-ray spectral analysis (CPD refers to cycle per day). The E_z exhibits the pattern of global thunderstorm activity of the Carnegie Curve along with an additional early morning peak typical of mountainous regions. Gamma-ray diurnal variations show a 24-h periodicity, with an average count rate of 220–230 counts/15 min. (For interpretation of the references to colour in this figure legend, the reader is referred to the web version of this article.)

down to the eastern Mediterranean. That system transported tropical air toward the Levant region at lower-levels of the atmosphere. In the upper-levels, a pronounced trough was situated west of the Levant. The storm developed off the Egyptian coastline near Alexandria and moved north-west, crossing the Israeli coast just north of Tel-Aviv on October 25, 2015 at 0900 local time. Deep convective cells developed rapidly, with thunderclouds exhibiting cloud top temperatures colder than $-70 \text{ }^\circ\text{C}$ (17 km) and radar reflectivity cores $> 65 \text{ dBz}$ at 10 km, which were accompanied by intensive lightning activity, severe hail,

downbursts and high rain rates. The entire episode terminated within 2 h as the super-cell subsided when reaching the Sea of Galilee in north-eastern Israel. $> 17,000$ cloud-to-ground lightning strokes were registered by the ILDN during this thunderstorm. A second phase of convective activity and lightning was around 1200 UT in the vicinity of Mt. Hermon. During these 24 h there were three distinct rain episodes near the mountain, where a clear departure from background values was observed in gamma counts and E_z values (Fig. 7b). The computed exponential half-lives depletion times (Fig. 7c) showing excellent fit

Table 1

Summary of the distinct events from October–November 2015 which were analyzed. In all events several precipitation episodes occurred in succession over Mt. Hermon station, while we separate between those events that exhibited lightning activity and those that were not accompanied by electrical activity. Highlighted grey row indicate events which were not taken into account when calculating mean gamma-ray increase or half-life times due to unsatisfactory fit ($R^2 < 0.95$) between the computed exponential half-life decay times and radioactive decay curves.

	Event time	Gamma enhancement duration	Gamma increase relative to background levels	Gamma return to normal background levels	E_z polarity change duration	Rain precipitation	Extracted half-life time decay	Number of lightning detected
1.	7/10/15 02:45–12:00 LT	~9 h	315 min	195 min	5.11 min, 6.54 min, 46.27 min	2 mm/3h, 2.4 mm/2h	47.15 min	---
2.	7/10/15 16:00–20:30 LT	~4.5 h	90 min	180 min	9.30 min	2.4 mm/3h	43 min	---
3.	7–8/10/15 22:15–02:00 LT	~4 h	60 min	180 min	2.31 min, 8.54 min, 7.09 min,	0.6 mm/h	53.7 min	---
4.	8/10/2015 02:00–04:30 LT	~2.5 h	45 min	105 min	3.28 min	6.7 mm/2h	57.7 min	---
5.	8/10/2015 04:30–09:00 LT	~4.5 h	75 min	250 min	6.08 min, 2.22 min	2.2 mm/2h	138.63 min ($R^2 < 0.95$)	---
6.	8–9/10/2015 21:30–02:30 LT	~5 h	90 min	210 min	5.01 min, 8.56 min	1.8 mm/4h	64.8 min	---
7.	9/10/2015 08:45–11:45 LT	~3 h	105 min	75 min	6.31 min	---	24.8 min	---
8.	9/10/2015 11:45–16:45 LT	~4 h	75 min	165 min	8.08 min, 5.36 min	2 mm/2h	55.4 min	---
9.	25/10/2015 09:00–20:00 LT	~11 h	30 min following 90 min	150 min	50.48 min	1.2 mm/2h, 12.6 mm/3h, 7.6 mm/3h	60.8 min	67
10.	28/10/2015 15:15–18:30 LT	~3 h	30 min	135 min	16.47 min (at 14:25)	9 mm/3h	82.51 min	86
11.	29/10/2015 07:00–11:30 LT 12:15–14:45 LT	~4.5 h, ~2.5 h	60 min, 30 min	90 min	7.16 min, 7.55 min	2.4 mm/2h, 0.8 mm/h	96.27 min	8
12.	16/11/2015 10:45–15:45 LT	~5 h	135 min, 30 min	105 min	3.25 min	3.2 mm/h	101.93 min	157 wvln/ 174 iec
13.	17/11/2015 06:15–10:00 LT 15:00–18:45 LT	~3.75 h, ~3.75 h	30 min, 45 min	165 min, 180 min	1.04 min, 4.10 min, 3.54 min	6 mm/2h, 1.6 mm/2h	54.57 min, 80.59 min	48

Bold refers to events of rain with lightning.

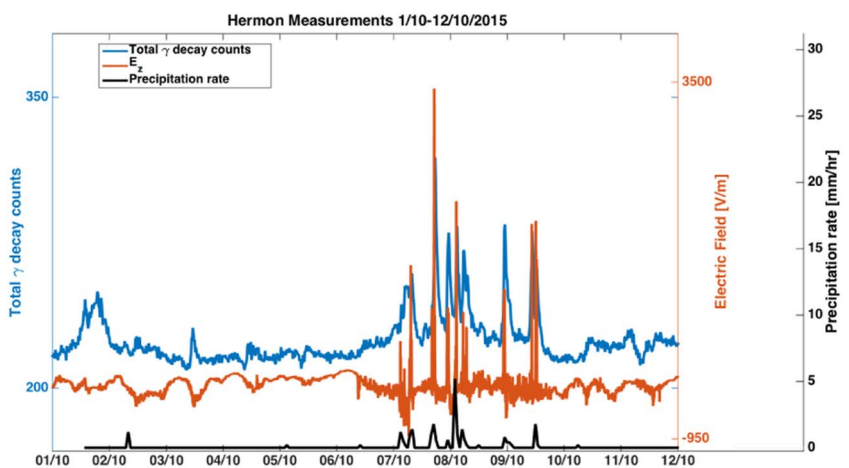


Fig. 3. Events of rain without lightning. October 1–12/2015 time series of the rainfall rate (black), the vertical component of the electric field (orange) and the gamma-ray counts (blue). (For interpretation of the references to colour in this figure legend, the reader is referred to the web version of this article.)

($R^2 > 0.98$) to radioactive depletion curves of 60.8 min. The electric field intensified up to a maximum value of 16,000 V/m. The episode of strongly disturbed E_z lasted ~50.48 min exhibiting polarity reversals instantaneously with the occurrences of 67 near-by CG lightning discharges.

4. Discussion

We show that the gamma-ray count rates observed by ground based NaI detectors in the 0.05–3 MeV range increase simultaneously with

changes in precipitation rates and vertical electric field intensification, during rain events with and without near-by CG lightning discharges. The correlation between gamma ray levels, precipitation and E_z without nearby lightning discharges is consistent with previous studies and models assuming that radon decay progenies are adsorbed predominantly on the surface of raindrops (Burnett et al., 2010; Greenfield et al., 2008, 2003). The gamma radiation increase is due to a combined effect of scavenging from the atmosphere of two solid radioactive isotopes, ^{214}Pb (half-life 26.8 min) and ^{214}Bi (half-life 19.9 min) (where ^{214}Pb decays to ^{214}Bi), exhibiting an exponential half-lives depletion

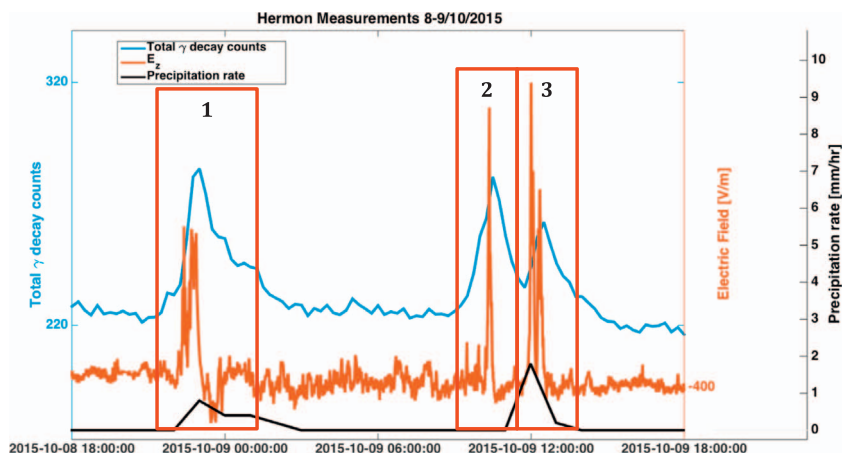


Fig. 4. Events of rain without lightning. Example of a slow increase (90 min) gamma ray enhancement (blue) accompanied by precipitation (black) and E_z enhancement (orange) during October 8–9, 2015. A clear departure from background values is observed in gamma counts and measured E_z values. (For interpretation of the references to colour in this figure legend, the reader is referred to the web version of this article.)

rate between ~25–65 min (with an average value of ~49 min). Furthermore, the fact that all the events were accompanied by relatively low rain-rates implies that the main process occurred during the fall of the raindrops through the air volume below the cloud-base (i.e. washout or rainout), presenting a higher scavenging efficiency per rain

drop compared with high rain-rates (because of the longer travel time). The intensification of the vertical electric field and its polarity reversals coincide with the time of increase in gamma-ray counts (relative to background levels) lasting ~105 min in average. This suggests that the cause of the E_z changes was a negatively charged cloud base passing

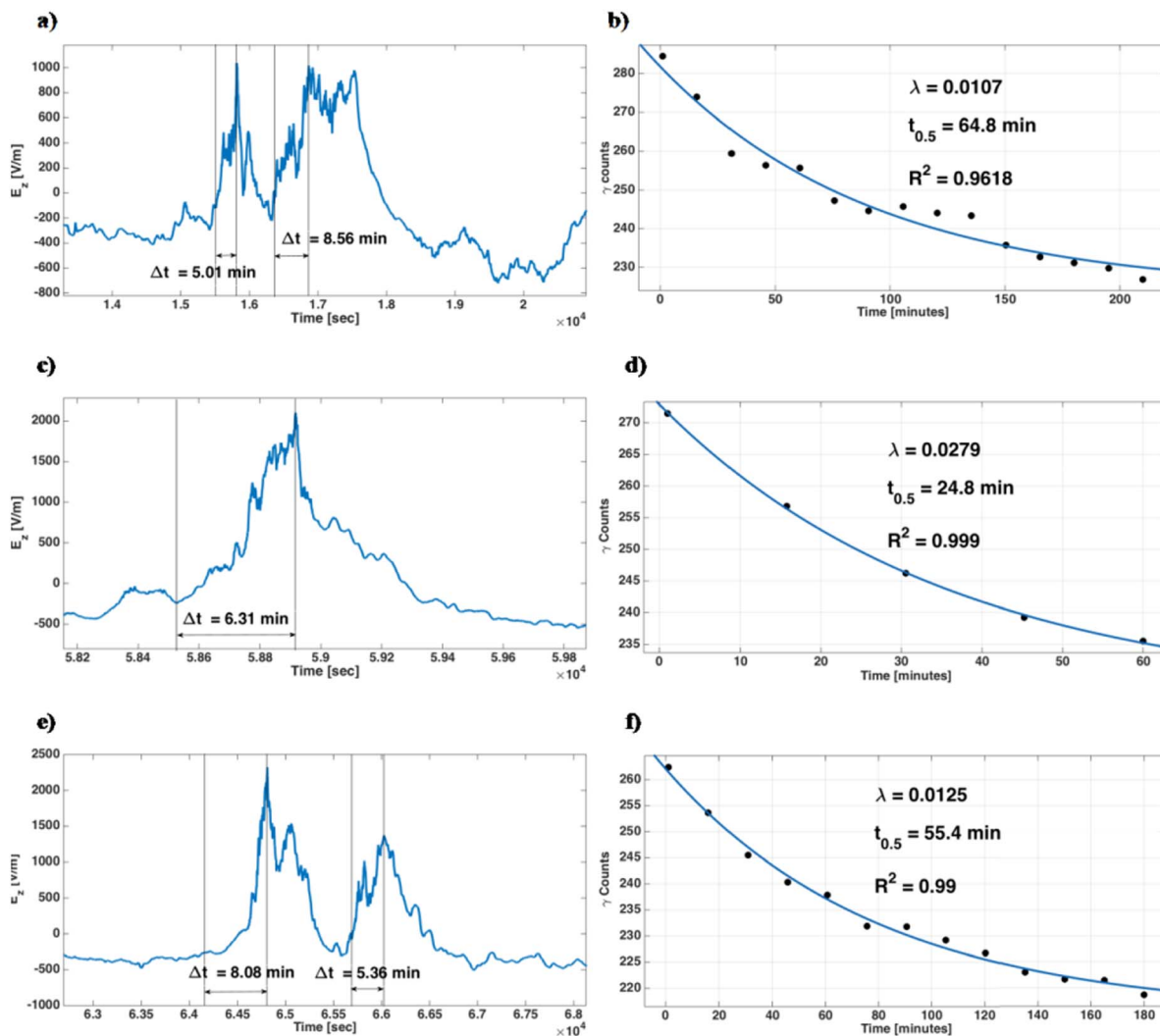


Fig. 5. E_z values (a, c and e) and computed exponential half-life depletion times (b, d and f) for red rectangle time periods 1–3 as indicated in Fig. 4. E_z values rises up to 2000 V/m on a time scale of a few minutes and returned to fair weather values quickly after the rain ceased. c). Computed exponential half-life decay times showing excellent fit ($R^2 > 0.96$) to radioactive decay curves of 64.8 (b), 24.8 (d) and 55.4 (f) minutes, thus indicating superposition of activity of radionuclides ^{214}Pb and ^{214}Bi being scavenge by the rain. (For interpretation of the references to colour in this figure legend, the reader is referred to the web version of this article.)

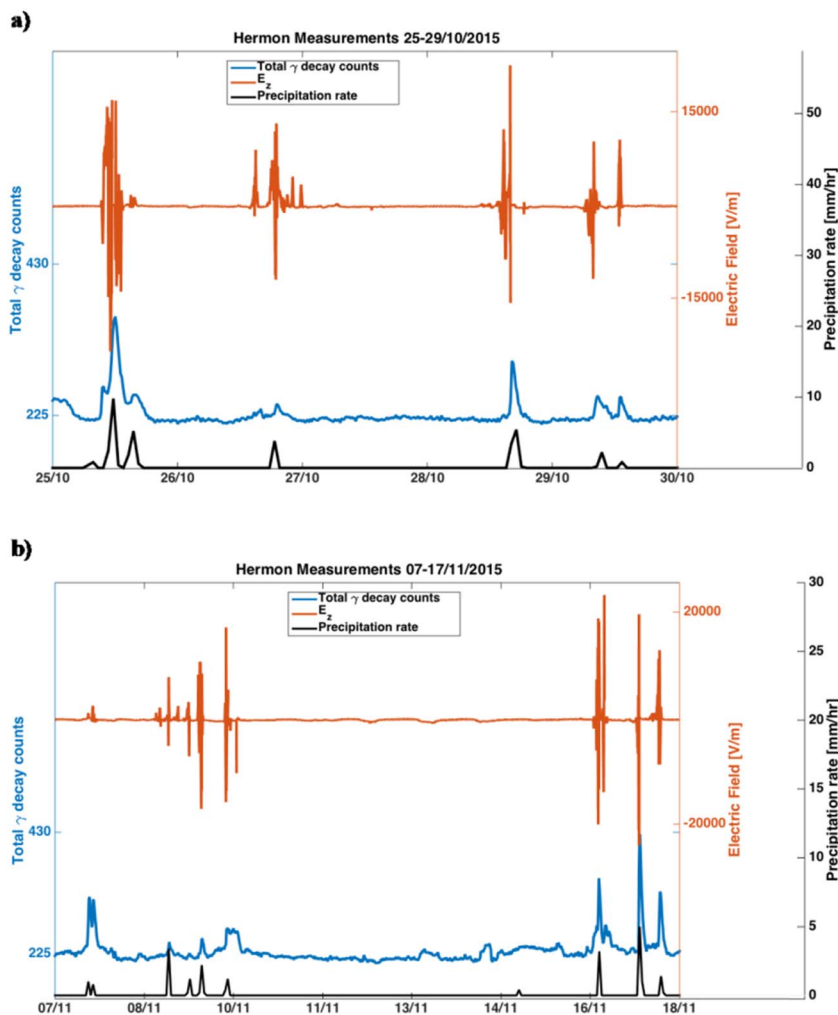


Fig. 6. Events of rain with lightning. a). October 25–30, 2015. b). November 7–18, 2015. Time series for the rainfall rate (black), the vertical component of the electric field (orange) and the gamma-ray counts (blue). (For interpretation of the references to colour in this figure legend, the reader is referred to the web version of this article.)

close to our station (Bennett and Harrison, 2008).

However, during events when lightning discharges were present, the gamma ray-precipitation- E_z correlation suggests a more complicated mechanism, involving other types of radioactive nuclides. The 30 min bursts of gamma-ray (compare to ~ 105 min in average for the events without lighting), along with minutes-scale E_z enhancements associated with the occurrence of near-by CG lightning discharges, is superimposed on the radiation from radionuclides scavenged by raindrops. The occurrence of lightning discharges after the minutes-range E_z reversals suggests the presence of a LPCR (a triple structure rather than the dipole structure of a main negative and positive charge centers) around our station (Williams, 1989). According to Chilingarian (2014) the strong electric fields within these clouds ($> 10^4$ V/m) operate as particle accelerators driving high-energy electrons (in the case of a strong positive electric field directed away from the earth) toward the surface, and when decelerated in the atmosphere they produce energetic gamma-rays (bremsstrahlung) directed toward the earth creating a detectable residual activity near the ground. The LPCR is significantly smaller than the main negative and positive charge centers and so the resultant electric fields in the lower part of the cloud are much weaker, which suggests a lower level of energies of accelerated electrons compared with the case of a strong negative electric field directed toward the surface. The cross section for bremsstrahlung is inversely proportional to the square of the accelerated particle's mass, and charge exchange reactions between the N_2 , O_2 and Ar molecules (that have fairly large cross sections) will cause observable activity only when the half-lives of the residual nuclei produced are between 10 and 100 min. Radioisotopes with shorter half-

lives will probably have decayed before reaching the ground (Greenfield et al., 2003).

5. Summary

In this study we report the detection of ground-level gamma-ray enhancements along with precipitation events and observed strong positive electric fields polarity reversals, for the first time at Mt. Hermon cosmic ray observatory in northern Israel. We distinguish between two types of events which were detected: slow increase of downward gamma ray radiation along with minutes-scale E_z enhancement, which were associated with weak rain-rates without the occurrences of near-by lightning, and a second type with fast bursts of gamma ray along with minutes-scale E_z enhancement and precipitation, which closely matched the occurrences of near-by lightning discharges. For the first type of events we deduce that the gamma-ray enhancements detected at ground were due to a combined effect of scavenging by precipitation (presumably washout effect) of two radioactive isotopes (^{214}Pb and ^{214}Bi) combined with E_z polarity reversal due to the fact that the cloud-base above the station is charged (Bennett and Harrison, 2007). For the second type of events we deduce a more complicated mechanism which involved acceleration of high-energy electrons due to the Lower Positive Charge Region (LPCR) electric fields in thunderstorms combined with radon progeny washout by precipitation.

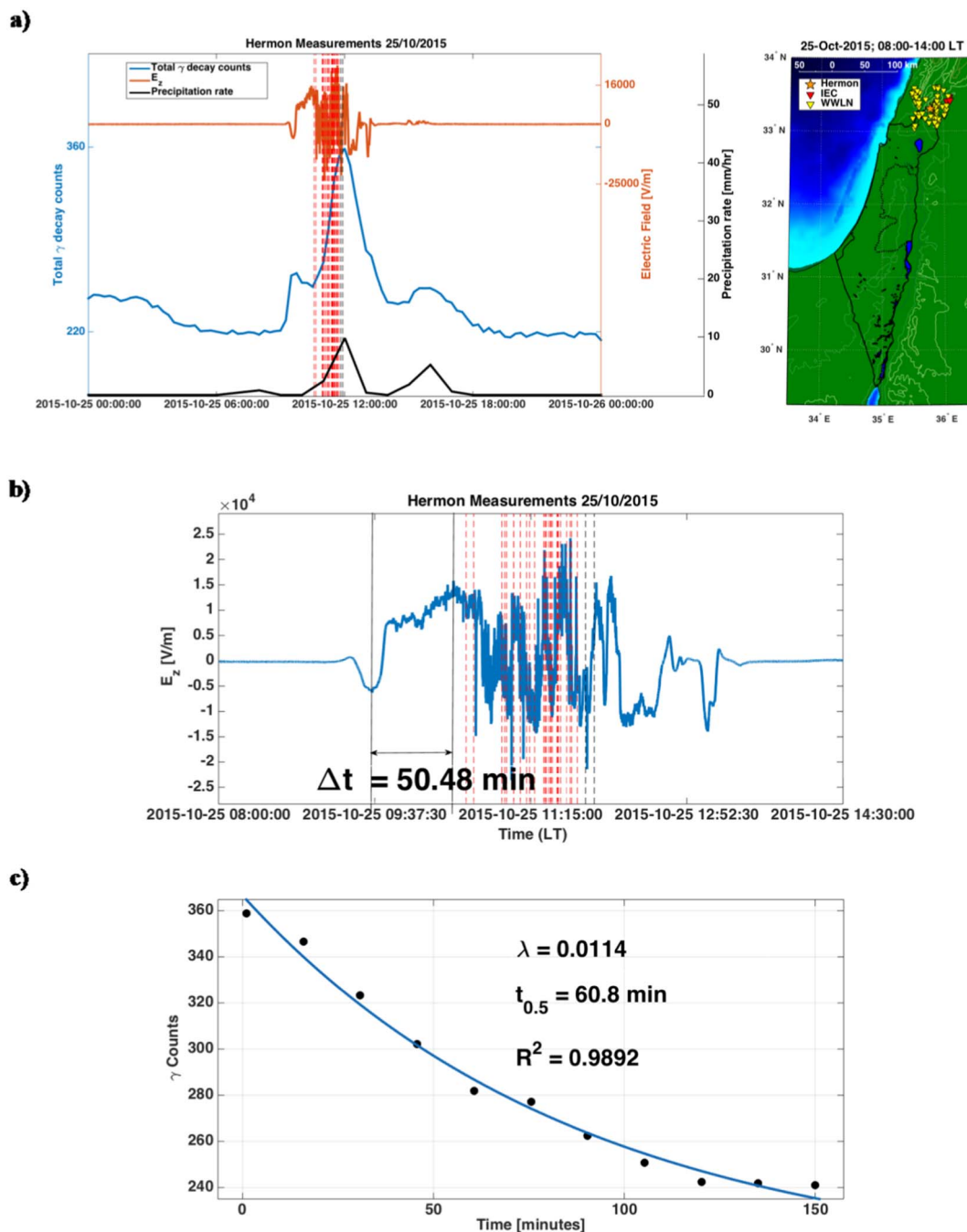


Fig. 7. a). Example of a fast increase (30 min) gamma ray enhancement (blue) along with minutes range E_z enhancement (orange), which closely matched the occurrences of 67 near-by CG lightning discharges, and are also accompanied by precipitation (black). The date is plotted along with the lightning activity (dash red lines) during the October 25, 2015 convective event. Red and yellow triangles on the map indicate the locations of the lightning taken from WWLNN and IEC networks. b). E_z values rises up to 16,000 V/m on a time scale of tens of minutes and returned to fair weather values quickly after the rain ceased. c). Computed exponential half-life decay times showing excellent fit ($R^2 > 0.98$) to radioactive decay curves of 60.8 min. (For interpretation of the references to colour in this figure legend, the reader is referred to the web version of this article.)

Acknowledgment

We wish to thank Roy Yaniv from Tel-Aviv University for helping with the E_z and J_z data acquisition. Special thanks are also due to Dr. Israel Silber for helping with the WWLNN data analysis. We also wish to thank Uri Malik from the Geological Survey of Israel (GSI) for helping in setting up the gamma-ray measurements at the site. This research is partially supported by the Israeli Science Foundation grant 423/14, and the Israeli Minister of Science, Technology & Space grant 3-13591.

References

Bennett, A.J., Harrison, R.G., 2007. Atmospheric electricity in different weather conditions. *Weather* 62 (10), 277–283.
 Bennett, A.J., Harrison, R.G., 2008. Surface measurement system for the atmospheric electrical vertical conduction current density, with displacement current density correction. *J. Atmos. Sol. Terr. Phys.* 70 (11), 1373–1381.
 Burnett, J.L., Croudace, I.W., Warwick, P.E., 2010. Short-lived variations in the background gamma-radiation dose. *J. Radiol. Prot.* 30 (3), 525.
 Chilingarian, A., 2014. Thunderstorm ground enhancements-model and relation to lightning flashes. *J. Atmos. Sol. Terr. Phys.* 107, 68–76.
 Chilingarian, A., Mkrtchyan, H., 2012. Role of the lower positive charge region (LPCR) in initiation of the thunderstorm ground enhancements (TGEs). *Phys. Rev. D* 86 (7), 072003.

- Cummins, K., Krider, E., 1998. The US National Lightning Detection Network/sup TM/ and applications of cloud-to-ground lightning data by electric power utilities. *IEEE Trans. Electromagn. Compat.* 40 (4), 465–480 (1998).
- Elhalel, G., Yair, Y., Nicoll, K., Price, C., Reuveni, Y., Harrison, R.G., 2014. Influence of short-term solar disturbances on the fair weather conduction current. *J. Space Weather Space Climate* 4, A26. <http://dx.doi.org/10.1051/swsc/2014022>.
- Fujinami, N., 1996. Observational study of the scavenging of radon daughters by precipitation from the atmosphere. *Environ. Int.* 22, 181–185.
- Greenfield, M.B., Domondon, A.T., Tsuchiya, S., Kubo, K., Ikeda, Y., Tomiyama, M., 2003. Near-ground detection of atmospheric γ rays associated with lightning. *J. Appl. Phys.* 93 (3), 1839–1844.
- Greenfield, M.B., Ito, N., Iwata, A., Kubo, K., Ishigaki, M., Komura, K., 2008. Determination of rain age via γ rays from accreted radon progeny. *J. Appl. Phys.* 104 (7), 074912.
- Harrison, R.G., 2013. The carnegie curve. *Surv. Geophys.* 34 (2), 209–232.
- Hirouchi, J., Hirao, S., Moriizumi, J., Yamazawa, H., Suzuki, A., 2014. Estimation of surface concentration of radon decay products from gamma dose rate change after rain. *Prog. J. Nucl. Sci. Technol.* 4, 871–874.
- Hornig, M.C., Jiang, S.H., 2004. In situ measurements of gamma-ray intensity from radon progeny in rainwater. *Radiat. Meas.* 38 (1), 23–30.
- Inomata, Y., Chiba, M., Igarashi, Y., Aoyama, M., Hirose, K., 2007. Seasonal and spatial variations of enhanced gamma ray dose rates derived from 222 Rn progeny during precipitation in Japan. *Atmos. Environ.* 41 (37), 8043–8057.
- Livesay, R.J., Blessinger, C.S., Guzzardo, T.F., Hausladen, P.A., 2014. Rain-induced increase in background radiation detected by Radiation Portal Monitors. *J. Environ. Radioact.* 137, 137–141.
- Mercier, J.F., Tracy, B.L., d'Amours, R., Chagnon, F., Hoffman, I., Korpach, E.P., Johnson, S., Ungar, R.K., 2009. Increased environmental gamma-ray dose rate during precipitation: a strong correlation with contributing air mass. *J. Environ. Radioact.* 100 (7), 527–533.
- Ringuette, R., Case, G.L., Cherry, M.L., Granger, D., Guzik, T.G., Stewart, M., Wefel, J.P., 2013. TETRA observation of gamma-rays at ground level associated with nearby thunderstorms. *J. Geophys. Res. Space Phys.* 118 (12), 7841–7849.
- Shalev, S., Saaroni, H., Izsak, T., Yair, Y., Ziv, B., 2011. The spatio-temporal distribution of lightning over Israel and the neighboring area and its relation to regional synoptic systems. *Nat. Hazards Earth Syst. Sci.* 11 (8), 2125–2135.
- Takeyasu, M., Iida, T., Tsujimoto, T., Yamasaki, K., Ogawa, Y., 2006. Concentrations and their ratio of (222)Rn decay products in rainwater measured by gamma-ray spectrometry using a low-background Ge detector. *J. Environ. Radioact.* 88, 74–89. <http://dx.doi.org/10.1016/j.jenvrad.2006.01.001>.
- Tsuchiya, H., Enoto, T., Yamada, S., Yuasa, T., Nakazawa, K., Kitaguchi, T., Kawaharada, M., Kokubun, M., Kato, H., Okano, M., Makishima, K., 2011. Long-duration γ ray emissions from 2007 and 2008 winter thunderstorms. *J. Geophys. Res.-Atmos.* 116 (D9).
- Williams, E.R., 1989. The tripole structure of thunderstorms. *J. Geophys. Res.-Atmos.* 94 (D11), 13151–13167.
- Yaniv, R., Yair, Y., Price, C., Mkrtychyan, H., Lynn, B., Reymers, A., 2017. Ground-based measurements of the vertical E-field in mountainous regions and the “Austausch” effect. *Atmos. Res.* 189, 127–133.
- Zafir, H., Haquin, G., Malik, U., Barbosa, S.M., Piatibratova, O., Steinitz, G., 2011. Gamma versus alpha sensors for Rn-222 long-term monitoring in geological environments. *Radiat. Meas.* 46 (6), 611–620.
- Zheng, H., Holzworth, R.H., Brundell, J.B., Jacobson, A.R., Wygant, J.R., Hospodarsky, G.B., Mozer, F.S., Bonnell, J., 2016. A statistical study of whistler waves observed by Van Allen Probes (RBSP) and lightning detected by WWLLN. *J. Geophys. Res. Space Phys.* 121, 2067–2079. <http://dx.doi.org/10.1002/2015JA022010>.